PINK1-dependent recruitment of Parkin to mitochondria in mitophagy

Cristofol Vives-Bauza[a,1], Chun Zhou[a,1], Yong Huang[a,1], Mei Cui[b], Rosa L.A. de Vries[a], Jiho Kim[c], Jessica May[a], Maja Aleksandra Tocilescu[a], Wencheng Liu[d], Han Seok Ko[e,f], Jordi Magrané[d], Darren J. Moore[e,f,2], Valina L. Dawson[e,f,g,h], Regis Grailhe[c], Ted M. Dawson[e,f,h], Chenjian Li[d], Kim Tieu[b], and Serge Przedborski[a,i,j,3]

Departments of [a]Neurology and [i]Pathology and Cell Biology and the [j]Center for Motor Neuron Biology and Disease, Columbia University, New York, NY 10032; [b]Department of Neurology, Center for Translational Medicine, University of Rochester, Rochester, NY 14642; [c]Institut Pasteur Korea, Gyeonggi-do 463-400, Republic of Korea; [d]Department of Neurology and Neurosciences, Weill Medical College of Cornell University, New York, NY 10065; [e]NeuroRegeneration and Stem Cell Programs, Institute for Cell Engineering, Departments of [f]Neurology and [g]Physiology, and the [h]Solomon H. Snyder Department of Neuroscience, Johns Hopkins University School of Medicine, Baltimore, MD 21205

Phosphatase and tensin homolog (PTEN)-induced putative kinase 1 (*PINK1*) and *PARK2/Parkin* mutations cause autosomal recessive forms of Parkinson's disease. Upon a loss of mitochondrial membrane potential ($\Delta\Psi_m$) in human cells, cytosolic Parkin has been reported to be recruited to mitochondria, which is followed by a stimulation of mitochondrial autophagy. Here, we show that the relocation of Parkin to mitochondria induced by a collapse of $\Delta\Psi_m$ relies on PINK1 expression and that overexpression of WT but not of mutated PINK1 causes Parkin translocation to mitochondria, even in cells with normal $\Delta\Psi_m$. We also show that once at the mitochondria, Parkin is in close proximity to PINK1, but we find no evidence that Parkin catalyzes PINK1 ubiquitination or that PINK1 phosphorylates Parkin. However, co-overexpression of Parkin and PINK1 collapses the normal tubular mitochondrial network into mitochondrial aggregates and/or large perinuclear clusters, many of which are surrounded by autophagic vacuoles. Our results suggest that Parkin, together with PINK1, modulates mitochondrial trafficking, especially to the perinuclear region, a subcellular area associated with autophagy. Thus by impairing this process, mutations in either *Parkin* or *PINK1* may alter mitochondrial turnover which, in turn, may cause the accumulation of defective mitochondria and, ultimately, neurodegeneration in Parkinson's disease.

autophagy | Parkinson's disease | phosphatase and tensin homolog-induced putative kinase 1

The common neurodegenerative disorder Parkinson's disease (PD) occasionally can be inherited (1, 2). Parkinson disease 6/phosphatase and tensin homolog (PTEN)-induced putative kinase-1 (PARK6/PINK1) is among the gene products associated with familial PD (2, 3). This 581-amino acid polypeptide is localized to the mitochondria and has only a single recognized functional domain, a serine/threonine kinase with a high degree of homology to that of the Ca^{2+}/calmodulin kinase family. Overexpression of WT PINK1 rescues abnormal mitochondrial morphology that has been described in *Drosophila* carrying *Pink1* mutations (4, 5), a finding that supports the notion that the mutated allele gives rise to a loss-of-function phenotype. Loss-of-function mutations in the gene encoding PARK2/Parkin (an E3 ubiquitin ligase) also can cause an autosomal recessive form of familial PD (2, 6). Parkin is thought to operate within the same molecular pathway as PINK1 to modulate mitochondrial dynamics (4, 5, 7). This possibility is intriguing, because Parkin has been reported to be essentially cytosolic (8, 9). However, we have shown that PINK1 spans the outer mitochondrial membrane, with its kinase domain facing the cytoplasm (10). These details of PINK1 topology are relevant to the reported Parkin/PINK1 genetic interaction because they place the only known functional domain of PINK1 in the same subcellular compartment as Parkin.

However, the role played by Parkin, PINK1, or both in mitochondrial dynamics is still uncertain. Perhaps, the beginning of an answer to this unresolved issue can be found in the recent study by Narendra et al. (9) in which they showed that, following a loss of mitochondrial membrane potential ($\Delta\Psi_m$), cytosolic Parkin relocates to the mitochondria (9). After this recruitment, mitochondrial depletion occurs through an autophagy-related gene 5 (*Atg5*)-dependent mechanism (9). These findings have led to the hypothesis that Parkin contributes to the removal of damaged mitochondria, an action that is essential to the well-being of neurons.

Given this mitochondrial Parkin-related effect and the reported Parkin/PINK1 interaction, we sought to determine whether PINK1 is involved in the recruitment of Parkin to the mitochondria and to define the role played by Parkin, PINK1, or both in mitochondrial turnover. Our work confirms that cytosolic WT but not mutated Parkin relocates to the mitochondria in response to a loss of $\Delta\Psi_m$ and also demonstrates that this phenomenon does not occur in the absence of PINK1. Furthermore, we show that overexpression of WT but not of mutated PINK1 is sufficient to trigger Parkin relocation to the mitochondria, even in cells with normal $\Delta\Psi_m$. We also show that co-overexpression of PINK1 and Parkin causes a collapse of the normal tubular mitochondrial network into mitochondrial aggregates and/or large perinuclear clusters. Many of these clusters are surrounded by a double-membrane structure that is positive for the autophagosome marker LC3 and the lysosome marker Lamp2. Based on these results, we propose a physiological scenario in which, once Parkin is recruited to the mitochondria by a PINK1-dependent mechanism, damaged mitochondria are delivered to the perinuclear area, where they are then degraded by autophagy. Because we have demonstrated that mutations in either Parkin or PINK1 impair this trafficking, neurodegeneration in these familial forms of PD may result from a defect in the turnover of dysfunctional mitochondria.

Protonophores Induce Parkin Relocalization to Mitochondria

Mounting evidence indicates that Parkin modulates mitochondrial dynamics and autophagy (4, 5, 7, 9). A prerequisite for Parkin's actions on mitochondria may be its translocation from the cytosol

to mitochondria, as shown after a dissipation of $\Delta\Psi_m$ with the protonophore carbonyl cyanide *m*-chlorophenylhydrazone (CCCP) in clonal cell lines (9). In the present study, we show that cytosolic Parkin translocates to mitochondria in transiently transfected embryonic kidney HEK293T cells, expressing YFP-tagged Parkin (Parkin-YFP), upon exposure to 10 μM of either CCCP or its analog, carbonyl cyanide *p*-trifluoromethoxyphenylhydrazone (FCCP) (Fig. S1). As in the study by Narendra et al. (9), we found that >150 out of 250 (>60%) of our analyzed transfected cells, rather than showing a normal diffuse Parkin-YFP fluorescence, exhibited 1 large or several smaller discrete Parkin-YFP spots after only 1-h exposure to these protonophores (Fig. S1*A*). Under these experimental conditions, >85% of these spots colocalized with the mitochondrial protein TOM20, and >65% of the mitochondria colocalized with Parkin after protonophore exposure, vs. ~10% after vehicle exposure (Fig. S1*B*). Identical results were obtained with GFP-tagged Parkin (Parkin-GFP) or c-Myc–tagged Parkin (Parkin-myc) and with *Parkin-YFP*–transfected human neuroblastoma SH-SY5Y and cervical carcinoma HeLa cells. In contrast to HeLa cells transfected with WT *Parkin* (*Parkin^WT*)-myc, cells transfected with mutated *Parkin^T415N*- or *Parkin^G430D*-myc, which are 2 PD pathogenic mutations (2), retained a normal diffuse cytosolic fluorescence whether cells were incubated with a protonophore or vehicle (Fig. 1*B*).

Dissipation of $\Delta\Psi_m$ Triggers Parkin Relocalization

To examine further the effect of protonophores on Parkin cytosolic/mitochondrial partition, we prepared subcellular fractions from both non–neuronal-like HEK293T and neuronal-like SH-SY5Y cells, as before (10). These experiments demonstrated that endogenous Parkin was enriched in the mitochondrial fractions after only 1-h exposure to 10 μM CCCP (Fig. S1*C*). Furthermore, we found that Parkin contained in mitochondrial extracts from cells treated with 10 μM CCCP was accessible to digestion with proteinase-K (Fig. 1*A*). This result indicates that, upon translocation, Parkin associates with the outer surface of the mitochondria. Concentrations of CCCP or FCCP in excess of 1 μM, as used by Narendra et al. (9) and by us here, can affect cellular functions other than $\Delta\Psi_m$ (11, 12). Nonetheless, as much as 30–50% of WT Parkin-YFP–transfected cells did show Parkin translocation to mitochondria triggered by mitochondrial depolarization, whether it was caused by lower concentrations of CCCP (10 nM–1 μM), by coincubation with 1 μM of the complex III inhibitor, antimycin A, plus 1 μM of the F_1F_0 ATPase inhibitor, oligomycin, or by a complete loss of mitochondrial respiratory function in Rho^0 cells (Fig. 1 *C* and *D*). In each of these 3 conditions, Parkin-YFP translocation to MitoTracker Deep Red-labeled mitochondria was observed in cells that consistently had the lowest $\Delta\Psi_m$ as assessed using tetramethyl rhodamine methyl ester (TMRM) fluorescence (Fig. 1*E*). Thus, these results provide further support to the notion that a marked mitochondrial depolarization triggers Parkin recruitment to the mitochondria. A loss of $\Delta\Psi_m$, as modeled here, is often regarded as a correlate to mitochondrial damage. If that correlation is valid, future studies will have to elucidate the actual nature of the mitochondrial damage that triggers Parkin relocalization.

Parkin Translocation Is PINK1-Dependent

Cereghetti et al. (13) have reported that mitochondrial depolarization also can stimulate the translocation of the fission protein Drp1 from the cytosol to the mitochondria through a calcineurin-dependent mechanism. Despite the apparent similarity between the Drp1 and Parkin observations, in our hands, the calcineurin inhibitor, cyclosporine A, failed to prevent CCCP-induced Parkin translocation (Fig. 1*D*), thus suggesting that Drp1 and Parkin translocation to mitochondria is governed by distinct molecular underpinnings. Given the reported Parkin/Pink1 genetic interaction observed in *Drosophila* (4, 5, 7) and our revised PINK1
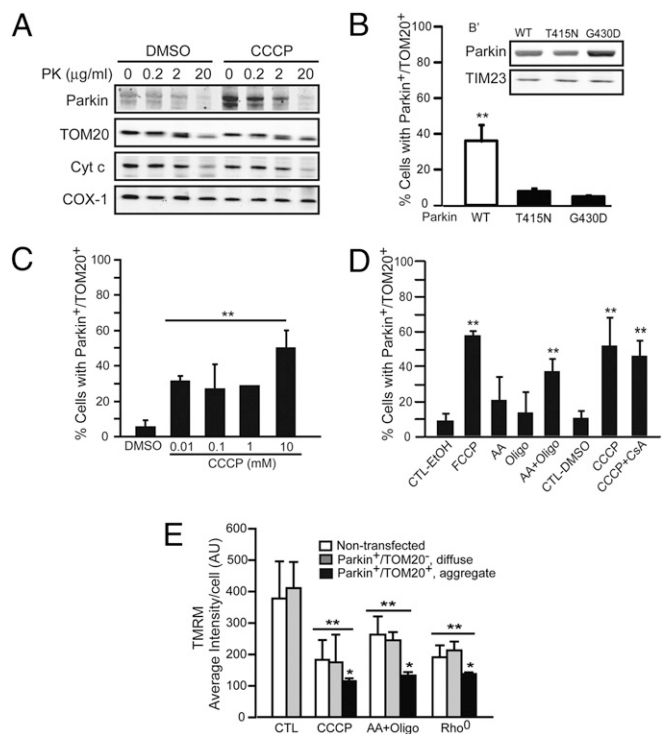

Fig. 1. Mitochondrial depolarization recruits WT Parkin to mitochondria. (*A*) Once recruited to mitochondria, Parkin associates with the mitochondrial outer membrane. HeLa cells were incubated with vehicle (DMSO) or with 10 μM CCCP for 1 h before mitochondrial isolation and protection assay by treatment with different concentrations of proteinase K (PK) (0, 0.2, 2, and 20 μg/mL). TOM20, cytochrome *c*, and COX-1 are markers of the outer membrane, intermembrane space, and inner membrane, respectively. (*B*) Parkin PD-linked mutant forms are not recruited to depolarized mitochondria. HeLa cells were transfected either with WT Parkin-myc or with mutant forms containing the pathogenic point mutations T415N and G430D. Twenty-four hours after transfection, cells were incubated with vehicle (DMSO) or with 10 μM CCCP for 1 h before fixation. Bars represent percent of cells showing Parkin-myc colocalization with TOM20 (Parkin$^+$/TOM20$^+$) ± SD of 3 independent experiments, determined by confocal microscopy. (*B'*) Western blot analysis shows that WT Parkin and its mutants T415D and G430P achieved comparable levels of protein expression. Parkin is immunodetected using anti-myc antibody. Loading is normalized by TIM23 (*C*) Effects on HeLa cells of 1-h incubation with different concentrations of CCCP, 24 h after transfection with Parkin-GFP. Bars represent percent of cells showing Parkin colocalization with TOM20 (Parkin$^+$/TOM20$^+$) ± SD of 3 independent experiments, determined by confocal microscopy. (*D*) Same as (*B*), but after 1-h incubation with 10 μM FCCP, 10 μM CCCP, 1 μM Antimycin A (AA), 1 μM Oligomycin (Oligo), or 1 μM AA and 1 μM Oligo (AA+Oligo) or after 30-min preincubation with 2 μM cyclosporine A (CsA), followed by 1-h incubation with 10 μM CCCP. Like FCCP and CCCP, AA+Oligo produce a significant percentage of cells with Parkin$^+$/TOM20$^+$. (*E*) Comparison of TMRM fluorescence acquired by live imaging and quantified as arbitrary units (A.U.) by Image J, among nontransfected and Parkin-GFP–transfected WT HeLa cells incubated with vehicle (CTL), 100 nM CCCP, or 1 μM AA + 1 μM Oligo and nontransfected and Parkin-GFP–transfected Rho^0 HeLa cells. Values represent mean ± SD (n = 35–50 cells) and are representative of 3 independent experiments. **, Different from CTL. *, Different from nontransfected and transfected cells with diffuse Parkin-GFP fluorescence (Newman–Keuls post hoc test; $P < 0.001$).

topology (10), we then asked whether PINK1 plays any role in the mitochondrial recruitment of Parkin. To address this question, we used a *PINK1* siRNA construct and HeLa cells, because we have previously shown that this reagent reduces *PINK1* mRNA by >80% in these specific cells (10). When *PINK1* was silenced in *Parkin^WT*-YFP–transfected HeLa cells, the CCCP-induced collapse of $\Delta\Psi_m$ was no longer associated with a relocalization of

cytosolic Parkin to the mitochondria (Fig. 2 A–C). A similar observation was made in primary cortical neurons from *Pink1*-knockout mice (Fig. 2D). The proto-oncogene DJ-1, when mutated, also causes a familial form of PD (2) and was suggested to interact with Parkin and PINK1 to form a mitochondrial multiprotein complex (14). However, unlike *PINK1* silencing, *DJ-1* knockdown by >75% in HeLa cells (Fig. 2B) had no effect on CCCP-mediated Parkin relocalization (Fig. 2C). Thus, whatever the functional nature of DJ-1 interaction with Parkin and PINK1 may be, our data exclude the possibility that DJ-1 is required for the PINK1-dependent translocation of Parkin to mitochondria.

PINK1 Causes Parkin Relocation in Cells with Normal $\Delta\Psi_m$

Next, we sought to determine the effect of increased PINK1 expression on $\Delta\Psi_m$ and Parkin subcellular distribution. To investigate this effect, we took advantage of stable rat fetal mesencephalic N27 cell lines developed by M.C. and K.T., which have an ecdysone-inducible mammalian expression system to regulate the expression of either human WT *PINK1* (*PINK1^{WT}*), 2 PD-linked *PINK1* mutants (the truncating nonsense mutation *PINK1$^{W437\times}$* and the missense mutation *PINK1^{L347P}*) (2), or, as control, an empty vector. These 4 cell lines, which share phenotypic similarities with dopaminergic neurons, were transfected transiently with Parkin-YFP as above and, 6 h later, were exposed to ponasterone A to induce the expression of human PINK1 (Fig. 3). In these cells, $\Delta\Psi_m$ was comparable to that of *Parkin-YFP*–

Fig. 2. *PINK1* knockdown prevents Parkin recruitment to depolarized mitochondria. (*A*) Immunofluorescence of HeLa cells cotransfected with Parkin-YFP and scrambled (scr) PINK1 or DJ-1 siRNA, and incubated for 1 h with 10 μM CCCP. Mitochondria are labeled with an anti-TOM20 antibody (red). (Scale bars, 10 μM.) Zoom shows 6× magnification of the region outlined by the box. (Scale bars, 1 μM.) (*B*) Effects of siRNA on PINK1 and DJ1 mRNA levels. Total RNA extracted from each sample is quantified by real-time PCR (*n* = 3). (*C*) Percentages of cells from the same set of cotransfected HeLa cells as in (*A*) that exhibit Parkin puncta colocalizing with the mitochondrial marker TOM20 (Parkin$^+$/TOM20$^+$). (*D*) Percentages of WT and knockout (KO) PINK1 cortical neurons that exhibit Parkin$^+$/TOM20$^+$ puncta following 1-h incubation with or without 100 nM CCCP. Values represent means ± SD (*n* = 30–50 cells) and are representative of 2–3 independent experiments. **, Different from controls (Newman-Keuls post hoc test; *P* < 0.001).

transfected/*PINK1*-noninduced and *Parkin-YFP*–transfected/ empty vector-induced cells (Fig. S2 *A* and *B*). However, despite having a normal $\Delta\Psi_m$—as evidenced by TMRM fluorescence in live-cell imaging (Fig. S2*A*)—cytosolic Parkin-YFP relocalized to the mitochondria at a time point corresponding to marked PINK1^{WT} induction (Fig. 3 *A*–*C*). Although the PINK1$^{W437\times}$ and PINK1^{L347P} cells had expression levels comparable to that of the PINK1^{WT} cells (Fig. 3*F*), no Parkin-YFP relocalization to the mitochondria was noted (Fig. 3 *D* and *E*). The effects of WT but not of mutated PINK1 on Parkin translocation were confirmed by *Pink1*/*Parkin-YFP* cotransfection in HeLa cells (Fig. S2*C*). We also transfected these cells with the artificial kinase dead mutant *PINK1^{K219M}*, which we showed to be overexpressed to comparable levels as *PINK1^{WT}* (10). Here, the proportion of cells overexpressing *PINK1^{K219M}* with Parkin-YFP relocalization (4.9 ± 3.0%, *n* = 100) was lower than that of cells overexpressing *PINK1^{WT}* (97.0 ± 1.4%, *n* = 100; Student's *t* test: *t*(198) = 27.7, *P* < 0.001). These results suggest that WT PINK1, but neither pathogenic nor functionally dead PINK1 mutants, is instrumental in the relocalization of cytosolic Parkin and operates downstream of mitochondrial depolarization.

Because both a loss of $\Delta\Psi_m$ and an increase in PINK1 expression promote Parkin translocation, we wondered if mitochondrial depolarization could enhance PINK1 expression. However, because CCCP triggers Parkin translocation within 1 h, we reasoned that any effect that a loss of $\Delta\Psi_m$ might have on PINK1 must be posttranslational in nature. Consistent with this view, we found, as before (10), that untreated HeLa cells were the only cells of the varied cell types used in this work in which endogenous mitochondrial PINK1 was detectable, albeit barely (Fig. 4), but endogenous PINK1 was seen clearly after 1-h exposure to 10 μM CCCP (Fig. 4). Remarkably, the mitochondrial contents of both full-length 63-kDa and cleaved 52-kDa PINK1 species increased after dissipation of $\Delta\Psi_m$, suggesting that mitochondrial depolarization may enhance PINK1 stability. Although the latter hypothesis may have to be tested formally in future studies, it has been reported that Parkin may indeed stabilize PINK1 (15).

Parkin Binds to PINK1 Without Modifying Each Other

The data presented in the previous sections raise the possibility that, once recruited to mitochondria, Parkin is physically apposed to PINK1, and this apposition may have important functional consequences. To ascertain this physical proximity, we used fluorescence lifetime imaging microscopy (FLIM) in living HEK 293T cells as reported previously (16). The fluorescence lifetime of CFP tagged at the C-terminus of PINK1 in transfected cells was 2.61 ± 0.04 ns (mean ± SEM; *n* = 7), but when cells were cotransfected with *Parkin-YFP*, the lifetime was reduced to 2.03 ± 0.03 ns (*n* = 4; Student's *t* test: *t*(9) = 8.57, *P* < 0.001; Fig. S3). However, when cells were cotransfected with *DJ-1-YFP* instead of *Parkin-YFP*, the lifetime of *PINK1-CFP* was unchanged, 2.61 ± 0.02 ns (*n* = 5; Student's *t* test: *t*(10) = 0.79, *P* = 0.449) (Fig. S3*A*). These results indicate that a positive energy transfer occurred specifically between PINK1-CFP and Parkin-YFP, supporting the close proximity of these 2 proteins.

We further assessed the physical proximity of Parkin and PINK1 by coimmunoprecipitation using human neuroblastoma SH-SY5Y cells [because these cells have relatively high levels of endogenous parkin (10)] stably transfected with a cDNA plasmid expressing full-length PINK1 tagged at the C-terminus with Flag (PINK1-Flag). On incubation of these cell extracts with a rabbit polyclonal anti-Parkin antibody (Abcam), endogenous Parkin immunoprecipitated, and PINK1-Flag did, also (Fig. S3*B*). Because of the lack of anti-PINK1 antibodies that reliably immunoprecipitate endogenous PINK1, it cannot be determined at present whether the immunoprecipitation of endogenous PINK1 can pull down Parkin.
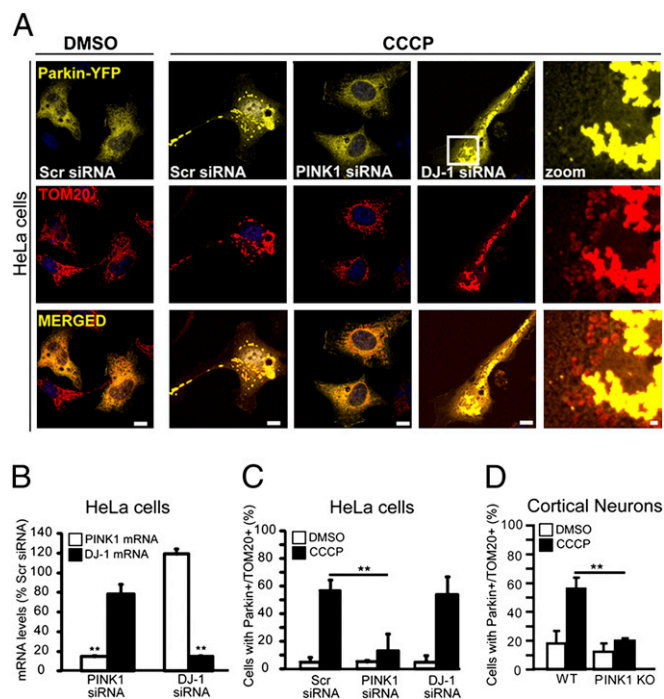
Fig. 4. Mitochondrial depolarization stabilizes both the 63-kDa full-length and the 52-kDa cleaved PINK1. Western blot analysis of the cytosolic and mitochondrial fractions of HeLa cells incubated for 1 hr with vehicle (DMSO), 10 μM CCCP, 1 μM Antimycin A (AA), 1 μM Oligomycin (Oligo), or the combination of 1 μM Antimycin A plus 1 μM Oligomycin (AA+Oligo). Treatments that dissipate $\Delta\Psi_m$, such as CCCP and AA+O, increase the PINK1 content in the mitochondrial fraction.
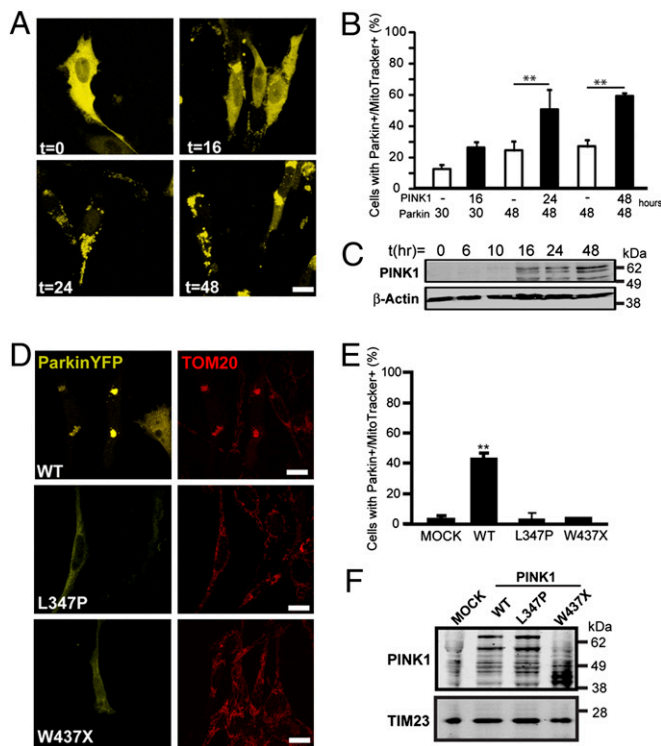
Fig. 3. Overexpression of PINK1 suffices to recruit Parkin to mitochondria with normal $\Delta\Psi_m$, as evidenced by TMRM fluorescence in living cells (see Fig. S2A). (*A*) Representative images illustrating the time-dependent changes in Parkin-YFP fluorescence from diffuse to punctate in immortalized mesencephalic neuronal N27 cells, after PINK1 induction. Parkin distribution is followed by live imaging of N27 cells expressing WT PINK1 driven by an inducible promoter. (Scale bar, 10 μM.) (*B*) Percentages of N27 cells showing Parkin translocation to mitochondria at selected time points after PINK1 induction and Parkin-YFP transfection. Mitochondria are labeled by MitoTracker Red. **, Different from non-induced N27 cells (Newman–Keuls post hoc test; P < 0.001). (*C*) Western blot from total cell extracts showing PINK1 induction over time. Loading is normalized with β-actin. (*D*) Representative images illustrating the recruitment of Parkin to mitochondria at 24 h after induction of WT PINK1 but not after induction of pathogenic PINK1 L347P and W437× mutants. (*E*) Percentages of N27 cells showing Parkin translocation to mitochondria at 24 h after induction of WT or mutant PINK1. Values represent means ± SD (*n* = 50 cells) and are representative of 3 independent experiments. **, Different from empty vector induction controls (Newman–Keuls post hoc test; P < 0.001). (*F*) Western blot from total cell extracts showing that PINK1 expression levels were comparable in WT PINK1 and PINK1 mutants L347P and W437×. Loading is normalized with TIM23.

suggest that Parkin and PINK1 may collaborate on some aspects of mitochondrial dynamics but probably not via posttranslational modification of each other.

Parkin/PINK1 Promotes Mitochondrial Clustering

Because we found that increased PINK1^{WT} expression suffices to recruit Parkin to the mitochondria, we assessed the effects of PINK1 and Parkin on mitochondrial distribution by over-expressing either or both proteins in SH-SY5Y cells to take advantage of their neuronal-like nature and their highly inter-connected tubular mitochondrial network. Once transfected, these cells were immunolabeled to detect EndoG and TOM20 as validated previously (10), and with MitoTracker 633. As expected, these different mitochondrial markers colocalized (Fig. S6). In untransfected cells and cells transfected with empty vectors, mitochondria appeared to be primarily tubular and organized in an interconnected network throughout the cell body, as expected (Fig. S6). Neither PINK1^{WT} nor Parkin^{WT} over-expression alone caused overt alteration of the mitochondrial network (Fig. 5*A*). In contrast, when SH-SY5Y cells were co-transfected with *PINK1^{WT}* and *Parkin^{WT}*, the normal mitochondrial network became altered. By 24–48 h after transfection, ~90% of the cells (*n* = 250) exhibited Parkin-positive fragmented mitochondria, primarily in the vicinity of the nucleus, and/or large, perinuclear clusters of MitoTracker-positive mitochondria (Fig. 5*A* and Fig. S6). Even at 48 h after transfection, ~10% of the cotransfected cells still had a normal tubular mitochondrial network (Fig. S6). Of note, in our pilot studies, we found that these changes in the mitochondrial network were similar to those observed in *Parkin*-YFP–transfected cells exposed to 10 μM CCCP for ~2 h. By co-overexpressing *Parkin^{WT}* and PD-linked mutated *PINK1* (A217D, G309D, L347P) or kinase dead mutant *PINK1^{K219M}* —all of which have markedly reduced kinase activities (17)—these mitochondrial changes were attenuated (Fig. 5*A* and Fig. S7). A similar observation was made with co-overexpression of functionally defective *Parkin* (produced by deletion of the RING2 domain) and *PINK1^{WT}* (Fig. S7). As confirmed by Western blots, in all the different combinations of coexpression, levels of mutated Parkin or PINK1 were at least comparable to those of their WT counterparts (Fig. 5*B*). These findings support the notion that the disruption of the mitochondrial network and the formation of mitochondrial aggregates and perinuclear clusters depend on both Parkin and PINK1 activity. We also found that the formation of perinuclear mitochondrial aggregates and clusters appeared to be specifically caused by Parkin and PINK1, because co-overexpression of *Parkin/DJ-1* and *PINK1/DJ-1* at comparable levels did not cause these mitochondrial structures (Fig. S7). Incidentally, we saw identical mitochondrial perinuclear phenotypes with *PINK1/Parkin* co-

These findings raise the possibility that Parkin may be a substrate for PINK1 or that PINK1 may be a client for Parkin. However, in our hands, we found no evidence of Parkin phosphorylation by PINK1 on [γ-^{32}P]ATP autoradiography or by use of phosphoserine- and phosphothreonine-specific antibodies (Fig. S4 *A* and *B*). We also found no electrophoretic indication that the phosphorylation status of Parkin extracted from mouse brain tissues was altered by the lack of Pink1 (Fig. S4C). To test the effect of Parkin on PINK1, Myc-PINK1, FLAG-Parkin, and HA-ubiquitin were coexpressed in SH-SY5Y cells (Fig. S5). This experiment showed that PINK1 was not covalently modified by HA-ubiquitin and that Parkin expression did not decrease the basal levels of PINK1. When these coexpressing cells were treated for 24 h with 5 μM of the proteasomal inhibitor MG132, there was no evidence that Parkin promoted the accumulation of PINK1-ubiquitin conjugates (Fig. S5B). Thus, we found that Parkin failed to ubiquitinate PINK1, to decrease its steady-state level, or to promote its proteasomal degradation. Collectively, these findings
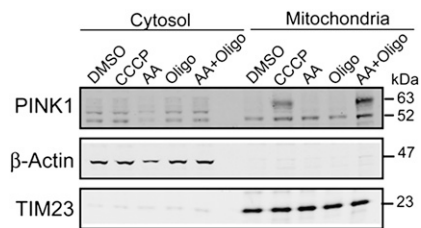
NEUROSCIENCE

overexpression in other cell lines, such as human neuroblastoma M17 and HEK 293T cells.

The Mitochondrial Clustering Is Microtubule-Dependent

The results reported in the previous sections support the view that Parkin and PINK1 may act in concert to modulate mitochondrial location, a complex function that typically relies on the microtubule motors (18). Consistent with this notion, in *PINK1*-stable SH-SY5Y cells transfected with *Parkin,* we found that >90% of the perinuclear mitochondrial clusters dispersed after only 1-h incubation with 1 µM nocodazole, a microtubule depolymerizing agent (Fig. S8A). Furthermore, in cells with perinuclear mitochondrial clusters, there was >80% colocalization between at least a part of these large perinuclear clusters and γ-tubulin, suggesting that they gather in the vicinity of the centrosome, an organelle that serves as the main microtubule-organizing center (Fig. S8B). However, we saw no obvious effect of nocodazole on the smaller perinuclear mitochondrial aggregates nor a definite colocalization between γ-tubulin and these mitochondrial aggregates. Further studies may be needed to elucidate whether these mitochondrial aggregates represent a distinct arrangement or a preceding stage [i.e., thanks to the microtubule motor, mitochondrial aggregates coalesce into larger perinuclear structures preferentially localized in the vicinity of the microtubule-organizing center, as supported by our time-lapse live imaging analyses (Video S1)]. Nonetheless, microtubules serve as railways for the transport of organelle cargos other than mitochondria (18). Remarkably, *PINK1/Parkin* co-overexpression seemed to modulate mitochondrial location specifically, because other microtubule organelle cargos, such as endoplasmic reticulum, never showed any change in their cellular organization (Fig. S9A). Thus, the interaction between PINK1 and Parkin may operate collaboratively on specific molecules of the mitochondrial trafficking machinery. In keeping with this idea is the demonstration that PINK1 can interact with the
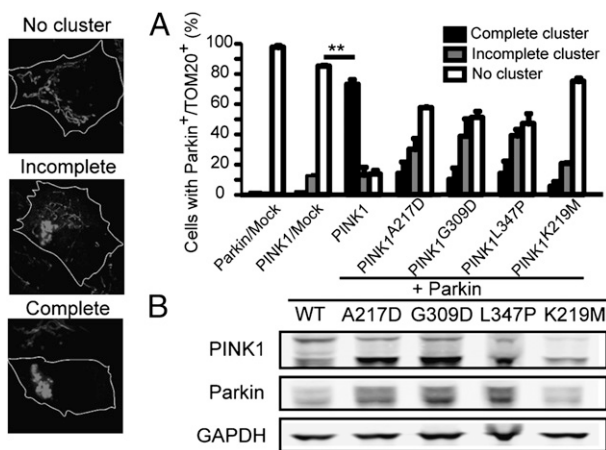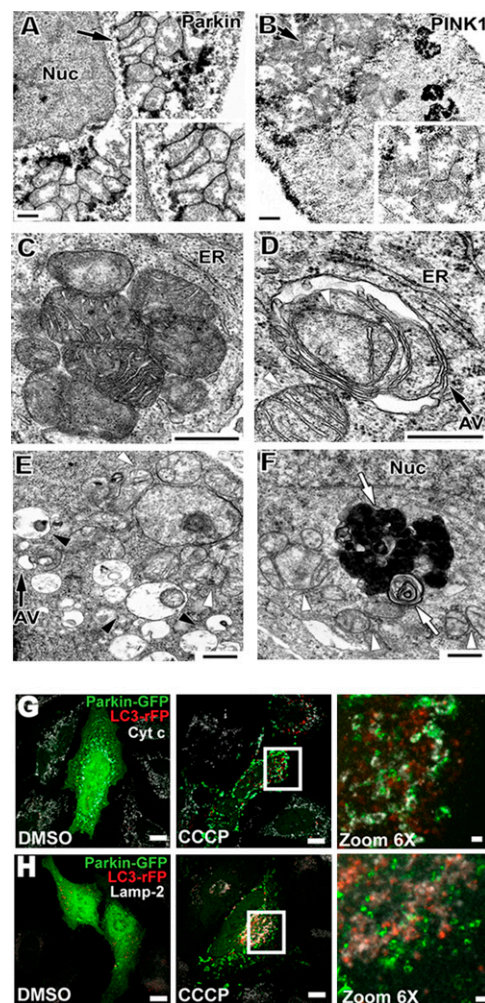

Fig. 6. Perinuclear mitochondrial clusters undergo mitochondrial autophagy. (*A–F*) SH-SY5Y cells cotransfected with Parkin and PINK1 were fixed and processed for EM with anti-Parkin or anti-PINK1 immunostaining (*A*, *B*) or without immunostaining (*C*, *D*). (*A*, *B*) With HRP-labeled secondary antibodies, immuno-EM showed perinuclear mitochondrial clusters (*arrows*), and both Parkin and PINK1 localized to the periphery of both individual mitochondrion (*Insets*) and fused mitochondria, consistent with immunofluorescent data that showed their colocalization (this figure and Fig. S5). (*C*) In some clustered mitochondria, mitochondrial outer membranes of 2 opposite mitochondria disappeared or fused but their inner membranes remained intact. (*D*) The autophagic vacuoles (AV) that contain mitochondria (*white arrowhead*) were found in the perinuclear area. (*E*, *F*) A mixture of clustered mitochondria (*white arrowhead*), autophagic vacuoles (*black arrowhead in E*), lysosomes (*white arrow in F*), and other nontypical vacuoles in the autophage–lysosome pathway (*black arrow in E*) are identified at the perinuclear area. (Scale bars, 500 nm.) (*G*, *H*) Immunofluorescence of HeLa cells transiently cotransfected with Parkin-GFP and LC3-rFP incubated with vehicle DMSO or CCCP for 1 h before cell fixation. In the perinuclear area where mitochondrial clusters accumulate, Parkin-GFP colocalized with LC3-rFP (*G*) and with Lamp-2 (*H*). (Scale bars, 10 µm.) Zoom denotes a 6× magnification of the region outlined by the box in the CCCP images. (Scale bars, 1 µm.). ER, endoplasmic reticulum; Nuc, nucleus.

Fig. 5. PINK1 PD mutations mitigate the formation of perinuclear mitochondrial clusters. (*A*) Three types of mitochondrial network morphology are defined in Parkin- and PINK1-cotransfected cells: no cluster (i.e., normal mitochondrial tubular network and distribution); incomplete cluster (i.e., mixture of perinuclear clustered mitochondria and dispersed linear mitochondria); and complete cluster (i.e., all mitochondria are clustered at the perinuclear area). Cells cotransfected with WT *Parkin* and *PINK1* show mainly complete clusters while cells cotransfected with WT *Parkin* and *PINK1* disease mutations or artificial dead kinase mutation (K219M) show mainly incomplete or no clusters. Bars represent percentage of cells for each type of mitochondrial morphology ± SEM; $n = 200$ cells counted during 3 independent experiments. **, Different from PINK1/Mock (Newman–Keuls post hoc test; $P < 0.01$). (Scale bars, 5 µm.) (*B*) Western blot from total cell extracts showing that Parkin and PINK1 expression levels were comparable in WT PINK1 and PINK1 mutants L347P and W437×. Parkin is immunodetected using anti-myc antibody. Loading is normalized with GAPDH.

mitochondrial protein Miro and the adaptor protein Milton (19), which connects kinesin heavy chain to Miro on mitochondria. However, our view of Parkin/PINK1 collaboration in mitochondrial trafficking in mammalian cells does not agree with the idea that, in *Drosophila*, Parkin operates downstream of Pink1 and that Parkin overexpression makes Pink1 dispensable (4, 5, 7). At this point, we cannot exclude the possibility that this apparent molecular divergence may result from an incomplete conservation of the Parkin/

PINK1 pathway between invertebrate and vertebrate organisms. It also should be taken into account that, here, we investigated the role of Parkin/PINK1 interaction on mitochondrial distribution and disposition, whereas in all the *Drosophila* studies the authors ascertained mitochondrial morphology and fission/fusion, very different aspects of mitochondrial dynamics that are not necessarily governed by an identical molecular machinery.

Parkin/PINK1 May Regulate Mitochondrial Trafficking

To examine the ultrastructure of perinuclear clustered mitochondria induced by Parkin/PINK1, we performed EM and observed a range of different types of mitochondrial perinuclear clusters that were not present in empty vector-transfected cells. In all cases, both the length and the width of perinuclear-clustered mitochondria in *Parkin*/*PINK1*-cotransfected cells were smaller than in mock-transfected control cells (Fig. S9B), suggesting that Parkin/PINK1 coexpression distorts the mitochondrial network, perhaps by promoting mitochondrial fragmentation. Furthermore, in some cases, clusters were made of nearly normal-appearing mitochondria, and both PINK1 and Parkin localized to the outside boundaries of each individual mitochondrion (Fig. 6*A* and *B*). In other cases, multiple mitochondria were fused together (Fig. 6 *A* and *C*). Among clustered mitochondria, the gap between 2 mitochondria was ~6 nm, similar to the gap of the mitochondria clusters induced by mitochondrial phospholipase-D (20). However, unlike mitochondrial phospholipase-D, Parkin/PINK1 overexpression was associated with mitochondrial outer-membrane fusion (Fig. 6*A*). We also identified perinuclear lysosomal vacuoles as well as autophagosomes, and some of these contained mitochondria (Fig. 6 *D* and *F*), suggesting a mitochondrial autophagic event. The autophagic nature of these vacuoles was confirmed by fluorescence for the autophagosome marker LC3-rFP and by immunofluorescence for the lysosome marker Lamp2 (Fig. 6 *G* and *H*). Notably, in untreated *Parkin-GFP*/*LC3-rFP* cotransfected cells, the LC3-rFP signal was detected throughout the cytoplasm (Fig. 6*G*). In contrast, in CCCP-treated cells, the LC3-rFP signal was localized mostly in the perinuclear region, where it colocalized with Parkin and the mitochondrial marker cytochrome *c* (Fig. 6*G*). Consistent with the preferential subcellular localization of lysosomes, Lamp2 immunofluorescence was detected primarily in the perinuclear area, which is the only subcellular region where we observed definite colocalization between Lamp2 and Parkin (Fig. 6*H*). Together

with our results for the microtubule experiments, these data suggest that autophagosomes containing Parkin/PINK1-enriched mitochondria may form at some distance from the lysosomes and then are delivered by the microtubule motor to the perinuclear lysosomes for degradation. This scenario is reminiscent of that proposed for the clearance of aggresomes (21), in which proteinaceous inclusion bodies are thought to be targeted to the perinuclear area to be disposed of by autophagy. Although our study is in agreement with that of Narendra et al. (9), in that we also found that cytoplasmic Parkin can translocate to the mitochondria, we argue that the ensuing autophagy of mitochondria requires the trafficking of damaged mitochondria to the perinuclear area to be degraded. We thus propose that both PINK1 and Parkin are key elements of the trafficking machinery responsible for delivering defective mitochondria to the lysosome-rich perinuclear area, rather than being part of the actual autophagy systems. The interplay between PINK1 and Parkin in mitochondrial functioning also may modulate the trafficking of mitochondria in dendrites, perhaps accounting for the synaptic dysfunction that is observed in PINK1- or Parkin-knockout mice (22, 23).

Materials and Methods

All methods employed in this article are routinely used in our laboratories and are thus referenced (10, 16, 24, 25) and are described in *SI Materials and Methods*. For immunoblotting, the primary antibodies used were PINK1 (100-494; Novus), Parkin, GAPDH, Hsp60, and HA (Santa Cruz Biotechnology), TIM23, cytochrome c, and COX-I (Invitrogen). For immunostaining, primary antibodies were PINK1 (Novus), myc (9E10; Abcam), EndoG (ProSci), TOM20 (BD Biosciences), α- and γ-tubulin (Sigma-Aldrich), calreticulin (AbCam), and tyrosine hydroxylase (Chemicon-Millipore).

1. Dauer W, Przedborski S (2003) Parkinson's disease: Mechanisms and models. *Neuron* 39:889–909.
2. Moore DJ, West AB, Dawson VL, Dawson TM (2005) Molecular pathophysiology of Parkinson's disease. *Annu Rev Neurosci* 28:57–87.
3. Valente EM, et al. (2004) Hereditary early-onset Parkinson's disease caused by mutations in PINK1. *Science* 304:1158–1160.
4. Clark IE, et al. (2006) Drosophila pink1 is required for mitochondrial function and interacts genetically with Parkin. *Nature* 441:1162–1166.
5. Park J, et al. (2006) Mitochondrial dysfunction in Drosophila PINK1 mutants is complemented by parkin. *Nature* 441:1157–1161.
6. Kitada T, et al. (1998) Mutations in the Parkin gene cause autosomal recessive juvenile parkinsonism. *Nature* 392:605–608.
7. Poole AC, et al. (2008) The PINK1/Parkin pathway regulates mitochondrial morphology. *Proc Natl Acad Sci USA* 105:1638–1643.
8. Darios F, et al. (2003) Parkin prevents mitochondrial swelling and cytochrome c release in mitochondria-dependent cell death. *Hum Mol Genet* 12:517–526.
9. Narendra D, Tanaka A, Suen DF, Youle RJ (2008) Parkin is recruited selectively to impaired mitochondria and promotes their autophagy. *J Cell Biol* 183:795–803.
10. Zhou C, et al. (2008) The kinase domain of mitochondrial PINK1 faces the cytoplasm. *Proc Natl Acad Sci USA* 105:12022–12027.
11. Zhang GJ, Liu HW, Yang L, Zhong YG, Zheng YZ (2000) Influence of membrane physical state on the lysosomal proton permeability. *J Membr Biol* 175:53–62.
12. Maro B, Marty MC, Bornens M (1982) In vivo and in vitro effects of the mitochondrial uncoupler FCCP on microtubules. *EMBO J* 1:1347–1352.
13. Cereghetti GM, et al. (2008) Dephosphorylation by calcineurin regulates translocation of Drp1 to mitochondria. *Proc Natl Acad Sci USA* 105:15803–15808.
14. Xiong H, et al. (2009) Parkin, PINK1, and DJ-1 form a ubiquitin E3 ligase complex promoting unfolded protein degradation. *J Clin Invest* 119:650–660.
15. Shiba K, et al. (2009) Parkin stabilizes PINK1 through direct interaction. *Biochem Biophys Res Commun* 383:331–335.
16. Grailhe R, et al. (2006) Monitoring protein interactions in the living cell through the fluorescence decays of the cyan fluorescent protein. *ChemPhysChem* 7:1442–1454.
17. Beilina A, et al. (2005) Mutations in PTEN-induced putative kinase 1 associated with recessive parkinsonism have differential effects on protein stability. *Proc Natl Acad Sci USA* 102:5703–5708.
18. Hirokawa N (1998) Kinesin and dynein superfamily proteins and the mechanism of organelle transport. *Science* 279:519–526.
19. Weihofen A, Thomas KJ, Ostaszewski BL, Cookson MR, Selkoe DJ (2009) Pink1 forms a multiprotein complex with Miro and Milton, linking Pink1 function to mitochondrial trafficking. *Biochemistry* 48:2045–2052.
20. Choi SY, et al. (2006) A common lipid links Mfn-mediated mitochondrial fusion and SNARE-regulated exocytosis. *Nat Cell Biol* 8:1255–1262.
21. Garcia-Mata R, Gao YS, Sztul E (2002) Hassles with taking out the garbage: Aggravating aggresomes. *Traffic* 3:388–396.
22. Goldberg MS, et al. (2003) Parkin-deficient mice exhibit nigrostriatal deficits but not loss of dopaminergic neurons. *J Biol Chem* 278:43628–43635.
23. Kitada T, et al. (2007) Impaired dopamine release and synaptic plasticity in the striatum of PINK1-deficient mice. *Proc Natl Acad Sci USA* 104:11441–11446.
24. Vives-Bauza C, et al. (2008) The age lipid A2E and mitochondrial dysfunction synergistically impair phagocytosis by retinal pigment epithelial cells. *J Biol Chem* 283:24770–24780.
25. Nagai M, et al. (2007) Astrocytes expressing ALS-linked mutated SOD1 release factors selectively toxic to motor neurons. *Nat Neurosci* 10:615–622.

NEUROSCIENCE